Chemical Engineering Journal 155 (2009) 411–418

Contents lists available at ScienceDirect

Chemical Engineering Journal

journal homepage: www.elsevier.com/locate/cej

Operation viability and performance of solid oxide fuel cell fuelled by different feeds

P. Piroonlerkgul[a], W. Wiyaratn[b], A. Soottitantawat[a], W. Kiatkittipong[c], A. Arpornwichanop[a], N. Laosiripojana[d], S. Assabumrungrat[a,*]

[a] Department of Chemical Engineering, Faculty of Engineering, Chulalongkorn University, Phyathai Road, Wang Mai, Phatumwan, Bangkok 10330, Thailand
[b] Department of Production Technology Education, Faculty of Industrial Education and Technology, King Mongkut's University of Technology Thonburi, Bangkok 10140, Thailand
[c] Department of Chemical Engineering, Faculty of Engineering and Industrial Technology, Silpakorn University, Nakhon Pathom 73000, Thailand
[d] The Joint Graduate School of Energy and Environment, King Mongkut's University of Technology Thonburi, Bangkok 10140, Thailand

ARTICLE INFO

Article history:
Received 5 March 2009
Received in revised form 31 July 2009
Accepted 4 August 2009

Keywords:
Biogas
Solid oxide fuel cell
Non-isothermal
Operation viability
Modeling

ABSTRACT

The performances of solid oxide fuel cells (SOFCs) fed by different types of feed, i.e. biogas, biogas-reformed feed, methane-reformed feed and pure hydrogen, are simulated in this work. Maximum temperature gradient and maximum cell temperature are regarded as indicators for operation viability investigation whereas power density and electrical efficiency are considered as performance indicators. The change in operating parameters, i.e. excess air, fuel feed rate and operating voltage, affects both the performance and operation viability of SOFC, and therefore, these operating parameters should be carefully selected to obtain best possible power density and reasonable temperature and temperature gradient. Pure hydrogen feed offers the highest SOFC performance among the other feeds. Extremely high excess air is required for SOFC fed by biogas to become operation viable and, in addition, its power density is much lower than those of SOFCs fed by the other feeds. Methane-reformed feed offers higher power density than biogas-reformed feed since H_2 concentration of the former one is higher.

1. Introduction

With the increasing concern on environmental problems, many countries are pursuing efforts to develop more sustainable energy systems to replace conventional combustion heat engines. Solid oxide fuel cell (SOFC) power generation shows great promise to serve as an alternative in the near future. For SOFC, the chemical energy can be transformed directly into the electrical energy. Therefore, the energy loss in an SOFC is lower than that in the conventional heat engines. Furthermore, additional efficiency can be gained by incorporating a steam/gas turbine cycle to recover heat from the hot gas exhausted from the SOFC which is typically operated at high temperatures between 1073 and 1273 K. By the same reason, various types of fuel, e.g. methane, methanol, ethanol, natural gas, oil derivatives, can be directly used as fuel in SOFC. Biogas is also one of the interesting alternatives. It can be derived from an anaerobic digestion process. In this process, organic matter present in the variety of sources, e.g. wastewater, animal waste, is microbial consumed in the absence of oxygen. The composition of biogas derived from this process varies with its source. It mainly contains, on a dry basis, methane (55–65%), carbon dioxide (30–40%), nitrogen (1–10%), oxygen (<5%) and trace of sulfur [1]. By using biogas in power generation, zero greenhouse gas emission can be achieved since CO_2 released from the process could be consumed in the photo-synthesis of plant.

The presence of CH_4 in the feed gas (biogas) at the anode side of SOFC decreases the SOFC performance due to the carbon deposition and partial blocking of anode pore [2]. Pre-reformer should be installed to resolve this problem. According to the literature, pre-reforming of methane before feeding to SOFC can improve the power density [3]. The removal of CO_2 from biogas before feeding can also improve the power density of biogas-fuelled SOFC [4]. The presence of CO_2 in SOFC feed dwindles its performance owing to the effect of reverse water gas shift reaction (RWGS) [5]. Our recent works also reported that SOFC fed by pure H_2 derived from using a palladium membrane reactor can offer higher power density compared with SOFC fed by reformed gas [6]. Even if the power density is a vital technical term used in evaluating SOFC performance, heat generation in SOFC stack should also receive closer attention. With inappropriate operating conditions, some solid parts in an SOFC stack may be damaged due to extreme increase in its temperature. At the present state-of-the-art of SOFC, YSZ typically used as an electrolyte material, the maximum allowable temperature gradient is around 10 K cm^{-1} [7]. A selection of suitable feedstock for SOFC is also an interesting issue in thermal consideration. Although the use of pure H_2 as SOFC feed can offer high power density, its rapid

* Corresponding author. Tel.: +66 2 218 6868; fax: +66 2 218 6877.
E-mail address: Suttichai.A@chula.ac.th (S. Assabumrungrat).

1385-8947/$ – see front matter © 2009 Elsevier B.V. All rights reserved.
doi:10.1016/j.cej.2009.08.001

Nomenclature

A	SOFC stack active area (m^2)
E	electromotive force (V)
E_0	electromotive force at standard pressure (V)
F	Faraday constant (9.6495×10^4) ($C\,mol^{-1}$)
$F_{CH_4,eq}$	methane equivalent flow ($mol\,s^{-1}$)
h	heat transfer coefficient ($W\,m^{-2}\,K^{-1}$)
ΔH_i	heat of reaction for ith reaction ($J\,mol^{-1}$)
ΔH_{elec}	heat of reaction for electrochemical reaction ($J\,mol^{-1}$)
H	energy rate ($J\,s^{-1}$)
i	current density ($A\,cm^{-2}$)
K_{ref}	equilibrium constant for steam reforming reaction (Pa^2)
l_a	thickness of anode (μm)
l_c	thickness of cathode (μm)
L	thickness of electrolyte (μm)
N_k	molar flow rate of component k ($mol\,s^{-1}$)
p_k	partial pressure of component k (Pa)
r_i	reaction rate for ith reaction ($mol\,s^{-1}$)
r_{ref}	reaction rate for steam reforming reaction ($mol\,s^{-1}$)
R	gas constant (8.3145) ($J\,mol^{-1}\,K^{-1}$)
T	temperature (K)
U_f	fuel utilization
V	cell voltage (V)

Greek letters

η_{act}	activation loss (V)
η_{conc}	concentration loss (V)
η_{ohm}	ohmic loss (V)
$\upsilon_{k,i}$	stoichiometric coefficient of component k in ith reaction
$\upsilon_{k,elec}$	stoichiometric coefficient of component k in electrochemical reaction

Superscript

j	jth control volume

Subscripts

a	anode channel
ave	average
c	cathode channel
$elec$	electrochemical reaction
i	ith reaction
k	component
ref	reforming reaction
s	solid trilayer

electrochemical reaction may cause high temperature gradient in solid parts of SOFC.

One-dimensional analysis (1D analysis) is an attractive technique to investigate the thermal behavior of an SOFC stack. Sorrentino et al. [8] employed 1D analysis for investigating temperature and current density profiles along the flow direction of a planar SOFC fed by reformed gas. The results obtained from the simulation shows good agreement with the experimental results. The investigation on the operation of indirect internal reforming SOFC (IIR-SOFC) fed by methane employing 1D analysis is performed by Lim et al. [7]. The results indicated that the temperature gradient of SOFC is extremely high near the exit of the anode section (entrance of reforming section) due to high extent of endothermic steam reforming reaction. Several methods were proposed in this literature to minimize the temperature gradient of SOFC, i.e. reduction of catalyst activity, use of non-uniform distributed catalyst and operation under autothermal reforming.

Aguiar et al. [9] studied the thermal behavior of IIR-SOFC towards the change in catalyst activity, fuel inlet temperature, current density and operating pressure utilizing 1D analysis. It was concluded that the increase in operating pressure can diminish both temperature gradient and overall temperature of IIR-SOFC due to the inhibition in reforming reaction rate and the improvement of electrochemical reaction rate. The reduction of the SOFC temperature gradient by minimizing the catalyst activity was also given by Aguiar et al. [10]. With this idea, less active catalyst is used in the reforming chamber of IIR-SOFC and, therefore, the local cooling effect caused from the reforming reaction is inhibited. However, the local cooling also generates, causing from the reforming reaction of unreacted methane at the entrance of the anode chamber. The results indicated that considerable decrease in temperature gradient can be achieved by reducing reforming activity of catalyst in both reforming chamber and anode chamber.

As described above, the performance and thermal behavior of SOFC depend on the type of feedstock and operating conditions. In this study, the performance of SOFC is analyzed employing 1D analysis. The effect of operating voltage, inlet fuel flow rate and inlet air flow rate (in term of excess air) on maximum temperature gradient and maximum temperature of solid part in the SOFC stack, power density and electrical efficiency are investigated for four types of SOFC feedstock, i.e. biogas, biogas-reformed feed, methane-reformed feed and pure H_2. To consider the viability of the operation of SOFC, maximum acceptable temperature gradient and maximum acceptable cell temperature are set to $10\,K\,cm^{-1}$ and 1273 K, respectively.

2. Modeling

2.1. SOFC stack model

Electrochemical reaction is the reaction between fuel (H_2 and CO) and oxidizing agent (air or O_2). At the cathode section, oxygen is reduced to oxygen ions (Eq. (1)) which permeate via the solid electrolyte to react with the hydrogen fuel (Eq. (2)) at the anode section. Only hydrogen is assumed to react electrochemically with oxygen ions due to the fact that the H_2 electro-oxidation is much faster than the CO electro-oxidation [11] and the rate of WGS reaction is fast at high temperatures [12–14]. Ni–Yttria Stabilized Zirconia (YSZ), YSZ and LSM–YSZ are chosen as the materials in the anode, electrolyte and cathode, respectively, of the SOFC stack:

$$\tfrac{1}{2}O_2 + 2e^- \rightarrow O^{2-} \quad (1)$$

$$H_2 + 2O^{2-} \rightarrow H_2O + 2e^- \quad (2)$$

The calculations take place for each control volume in the flow direction of SOFC stack as described in Fig. 1. The open circuit voltage (E^j) of the cell can be calculated from the Nernst equation which is expressed as:

$$E^j = E_0^j + \frac{RT_s^j}{2F} \ln\left(\frac{p_{H_2}^j (p_{O_2}^j)^{1/2}}{p_{H_2O}^j}\right) \quad (3)$$

The actual cell potential (V) is always less than the open circuit voltage (E^j) due to the existence of overpotentials as shown in Eq. (4). The overpotentials can be categorized into three main sources: ohmic overpotential (η_{ohm}^j), activation overpotential (η_{act}^j) and concentration overpotential (η_{conc}^j). The details on the calculation of these three overpotentials given in our recent work [4] are also

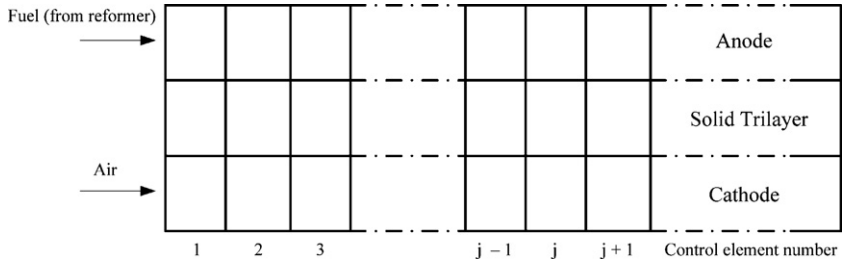

Fig. 1. A small element divided for the calculation in SOFC cell.

used in the present work:

$$V = E^j - \eta^j_{act} - \eta^j_{ohm} - \eta^j_{conc} \tag{4}$$

2.2. Mass and energy balance in SOFC stack

Mass and energy balance computations take place for each control volume (1 mm distance) in the flow direction of the SOFC stack. To simplify the problem, the following assumptions are made: (i) the pressure drop across the cell is neglected; (ii) heat radiation between solid components of the cell is negligible [8]; (iii) heat conduction in the solid electrolyte of the cell is neglected [8]. For pure-H_2 feed, only the electrochemical reaction (Eq. (2)) takes place in the cell anode side. However, for biogas, methane and reformed gas feed, steam reforming reaction (Eq. (5)) and WGS reaction (Eq. (6)) also occur in the anode side of the cell. Thermodynamic equilibrium is assumed for the WGS reaction in each region since its reaction rate is very fast at high temperature as described in Section 2.1. The rate of the reforming reaction in the SOFC stack [15] can be calculated employing Eq. (7) and the mass balance equations for each component in the anode and cathode sides are given in Eqs. (8) and (9), respectively:

$$CH_4 + H_2O \rightarrow CO + 3H_2 \tag{5}$$

$$CO + H_2O \rightarrow CO_2 + H_2 \tag{6}$$

$$r^j_{ref} = 4274A^j\, e^{-(82000/RT^j_s)} p^j_{CH_4} \left(1 - \frac{p^j_{CO}(p^j_{H_2})^3}{p^j_{CH_4} p^j_{H_2O} K^j_{ref}}\right) \tag{7}$$

$$N^{j+1}_{a,k} = N^j_{a,k} + \sum_i \nu_{k,i} r^j_i + \frac{\nu_{k,elec} i^j A^j}{2F} \tag{8}$$

$$N^{j+1}_{c,k} = N^j_{c,k} + \frac{\nu_{k,elec} i^j A^j}{2F} \tag{9}$$

A constant operating voltage along the cell length is assumed as the current collector usually has high electrical conductivity. For the energy calculation, excess heat produced in the solid trilayer caused from reactions (1) and (2) and the irreversibility of the electrochemical reaction is transferred to the anode and cathode channels. Energy balance equations for each small element in anode, cathode and solid trilayer are given in Eqs. (10)–(12), respectively:

$$H^{j+1}_a = H^j_a + h_a A^j (T^j_s - T^j_a) \tag{10}$$

$$H^{j+1}_c = H^j_c + h_c A^j (T^j_s - T^j_c) \tag{11}$$

$$-h_a A^j (T^j_s - T^j_a) - h_c A^j (T^j_s - T^j_c) + \left[\frac{(-\Delta H)^j_{elec}}{2F} - V\right] i^j A^j + \sum_i r^j_i (-\Delta H)^j_i = 0 \tag{12}$$

In the consideration, maximum temperature gradient and maximum temperature in the solid trilayer are determined and compared with maximum acceptable temperature gradient and maximum acceptable cell temperature. Also, the technical terms, i.e. average current density (i_{ave}), fuel utilization (U_f), electrical efficiency and excess air, are defined as follows:

$$i_{ave} = \frac{\sum_j i^j A^j}{\sum_j A^j} \tag{13}$$

$$U_f = \frac{(\sum_j i^j A^j / 2F)}{4F_{CH_4,eq}} \tag{14}$$

$$\%\text{electrical efficiency} = \frac{\text{electrical power}}{\text{LHV of SOFC anode feed} \times \text{anode feed rate}} \times 100 \tag{15}$$

$$\%\text{excess air} = \frac{0.21 \times \text{air feed rate}}{4F_{CH_4,eq}} \times 100 \tag{16}$$

It should be noted that for different types of feed, the feed rates are based on the same "methane equivalent flow ($F_{CH_4,eq}$)" as defined in Section 2.3. The term "excess air" stands for the flow rate of air fed into the SOFC system relative to the stoichiometric flow rate of air required for complete combustion of methane equivalent flow.

2.3. Type of feed in consideration

Four feed types, i.e. biogas, reformed-biogas, reformed-methane and pure-H_2, are considered in this study. Their compositions are determined by the following hypotheses:

Biogas: In this study, the quantity of methane and carbon dioxide in biogas is assumed to be fixed at 60 and 40%, respectively (biogas feed rate = $F_{CH_4,eq}/0.6$). Steam is fed together with biogas into the SOFC cell. The amount of steam is 2.5 times of methane in biogas.

Biogas-reformed feed: Biogas (biogas feed rate = $F_{CH_4,eq}/0.6$) and steam is fed into the reformer prior to be fed to SOFC cell. The quantity of steam fed is equal to that in case of biogas feed. Two chemical reactions, i.e. steam reforming (Eq. (5)) and WGS (Eq. (6)), take place in the reformer. Thermodynamic equilibrium is assumed for the calculation of reformer.

Methane-reformed feed: The calculation of SOFC feed composition for methane-reformed feed is identical to that for biogas-reformed feed; however, the reformer feed is changed from biogas to methane (methane feed rate = $F_{CH_4,eq}$).

Pure-H_2: H_2 is fed directly into SOFC cell. Its feed rate is equal to 4 times of $F_{CH_4,eq}$ (H_2 feed rate = $4 \times F_{CH_4,eq}$).

3. Results and discussion

All models used in this study are written in Visual Basic and the values of all parameters utilized in the computation are summa-

Table 1
Summary of model parameters [18,19].

Parameters	Value
SOFC cell	
l_a	750 μm
l_c	50 μm
L	50 μm
Cell length	400 mm
Cell width	100 mm
Anode channel height	1 mm
Cathode channel height	1 mm
$h_a = h_c$	0.2 kJ m^{-2} s^{-1} K^{-1}
Operating pressure	1 bar
SOFC feed temperature	998 K
Reformer	
Operating temperature	998 K
Operating pressure	1 bar

rized in Table 1. As described in our previous work [16], the SOFC model used in the calculation can well predict the experimental results of Zhao and Virkar [17] for the mixture of hydrogen (97%) and water (3%).

Temperature profiles of the solid part in SOFC fed by different feeds are first investigated. A base case is determined as given in Table 2. The operating voltage for each case is tuned up to achieve U_f = 80% at constant excess air and $F_{CH_4,eq}$. As described in Table 2, SOFC fed by pure-H_2 offers higher power density than the other feed types since it operates at higher operating voltage. Moreover, the maximum temperature gradient and maximum cell temperature of the pure-H_2 feed are much lower than those of the other feed types.

As illustrated in Fig. 2a, excluding SOFC fed by biogas, temperature of the solid part of SOFC increases along the flow direction due to the release of heat generated from irreversibility of the electrochemical reaction. The increase in temperature of the solid part of SOFC with the cell distance is more severe for the biogas-reformed feed and the methane-reformed feed compared with that of the pure-H_2 feed. It is obvious that the operation at high operating voltage can reduce irreversibility loss and also temperature gradient of solid part in the SOFC cell. For the SOFC fed by biogas, the decrease in cell temperature with cell distance is found at the inlet of the cell. This is due to the effect of the endothermic steam reforming reaction. Considering power density profile, power density increases with cell distance as shown in Fig. 2b. The increase in cell temperature along the cell distance causes the reduction of ohmic loss and consequently the power density increases. The increase in power density inside the SOFC cell fed by biogas-reformed feed and methane-reformed feed is more severe than in the case of pure-H_2 feed which is conformed to the increase of temperature with distance in Fig. 2a. However, near the gas outlet of the SOFC cell, the decrease in power density with cell distance is observed even if the increase in cell temperature with cell distance is observed. This implies that the effect of the depletion of H_2 concentration

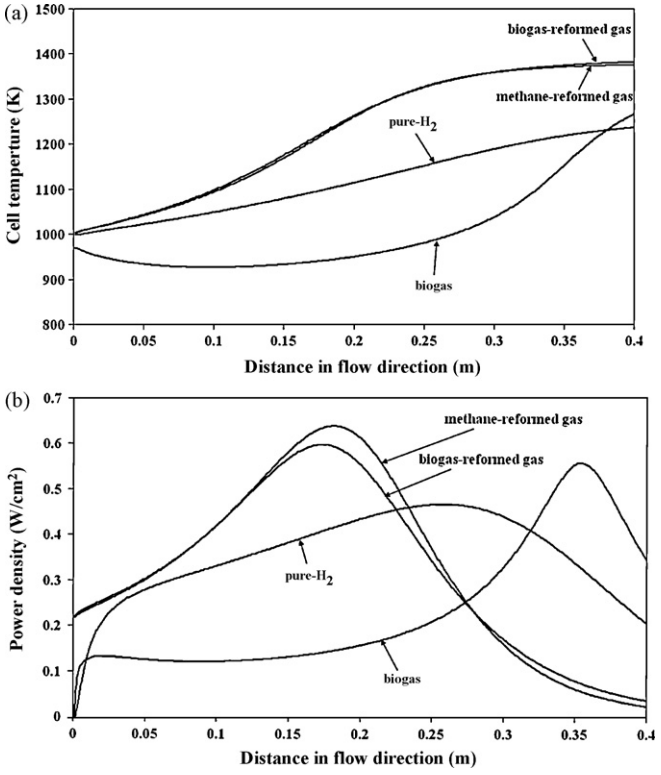

Fig. 2. The variation of (a) cell temperature and (b) power density with cell distance in SOFC cell fed by different types of feed. ($F_{CH_4,eq} = 3 \times 10^{-4}$ mol s^{-1}, excess air = 400%, U_f = 0.8).

with cell distance dominates the effect of the increase in cell temperature near the gas outlet of SOFC. Similar to the change in cell temperature in the flow direction, the decrease in power density of SOFC fed by biogas with cell distance is observed at the gas inlet of the SOFC cell.

The effect of the change in excess air on the maximum temperature gradient and maximum cell temperature of the solid part of SOFC fed by different types of feed is investigated as illustrated in Fig. 3a. As excess air increases, maximum temperature gradient and maximum temperature of the solid part in SOFC cell decrease, implying that SOFC is more feasible to operate at high excess air. However, using large amount of oxidizing agent (air), massive air compressor is required and much of electricity generated in SOFC must be supplied to it. Hence, the appropriate excess air value should be carefully selected. Even if the operation with high excess air can improve the operation viability (lower temperature gradient) of SOFC, the power density and fuel utilization are inhibited for SOFC fed by pure-H_2 as shown in Fig. 3b. This is due to the decrease in cell temperature which results in the increase in ohmic loss as excess air increases. Inversely, the power density and fuel utiliza-

Table 2
Base case in consideration for different feed (U_f = 0.8).

Type of feed	Biogas	Biogas-reformed feed	Methane-reformed feed	Pure-H_2
$F_{CH_4,eq}$ (mol s^{-1})	0.0003	0.0003	0.0003	0.0003
Excess air (%)	400	400	400	400
Operating voltage (V)	0.511	0.695	0.714	0.769
Power density (W cm^{-1})	0.234	0.322	0.33	0.357
Current density (A cm^{-1})	0.457	0.463	0.463	0.464
Electrical efficiency (%)	38.86	42.74	44.51	49.14
U_f	0.8	0.8	0.8	0.8
Electricity produced (W)	93.53	128.67	132.12	142.61
Maximum temperature gradient (K cm^{-1})	28.75	18.08	18.65	7.68
Maximum cell temperature (K)	1267.5	1381.5	1375.7	1236.6

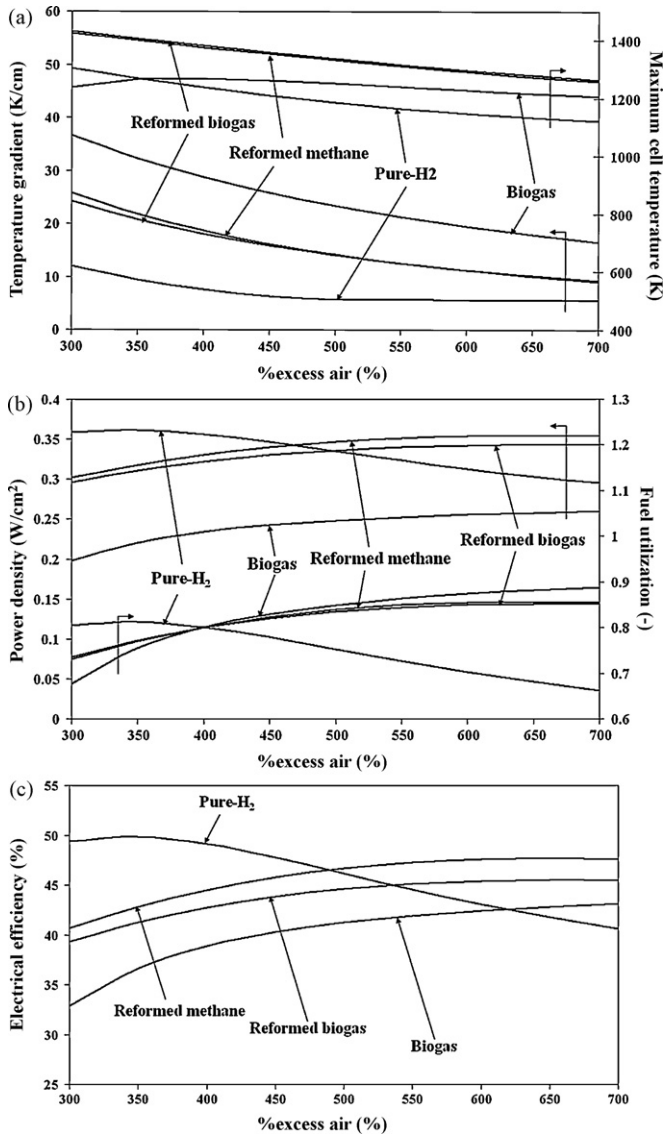

Fig. 3. The effect of the change in excess air on (a) the maximum temperature gradient, maximum cell temperature, (b) power density, fuel utilization and (c) electrical efficiency for SOFC fed by different types of feed. ($F_{CH_4,eq}$ and operating voltage are equal to base case values.)

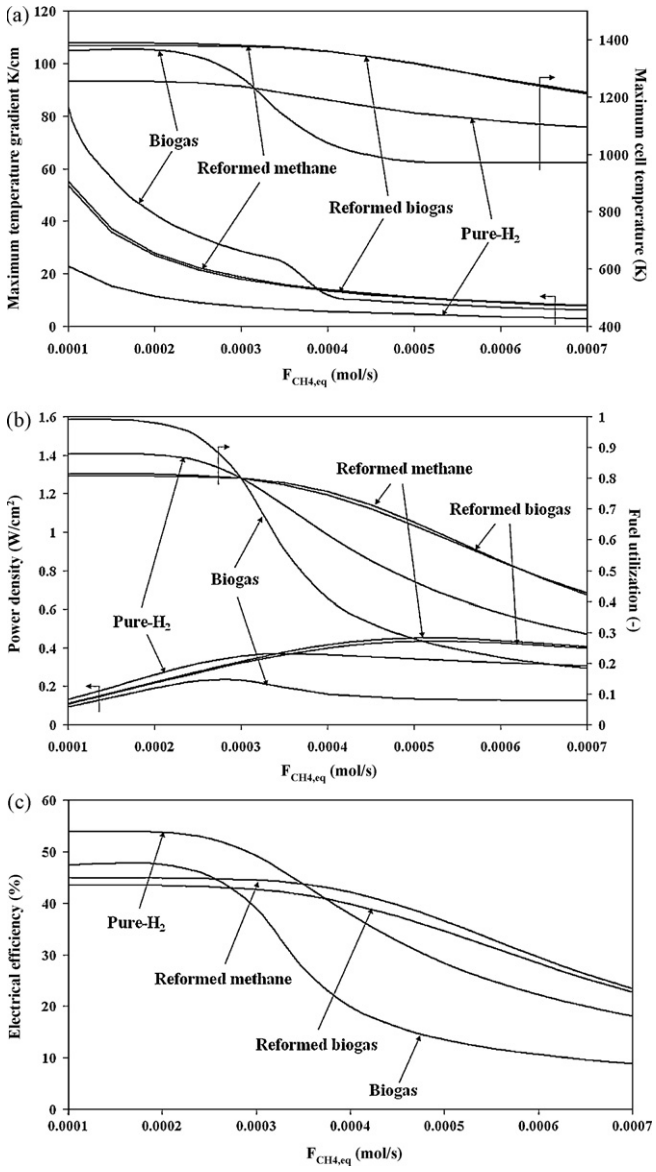

Fig. 4. The effect of the change in $F_{CH_4,eq}$ on (a) the maximum temperature gradient, maximum cell temperature, (b) power density, fuel utilization and (c) electrical efficiency for SOFC fed by different types of feed. (Excess air and operating voltage are equal to base case values.)

tion obtained from biogas-reformed feed, methane-reformed feed and biogas increases with the increase in excess air. This is due to the effect of the increase in electromotive force as the cell temperature decreases could defeat the effect of the increase in ohmic loss. The influence of excess air on the electrical efficiency of SOFC stack is also studied as illustrated in Fig. 3c. Similar to power density and fuel utilization, optimum electrical efficiency is found at low % excess air for SOFC fed by pure-H_2 and the electrical efficiency increases with excess air for SOFC fed by the other feeds.

Fig. 4a shows effect of the change in $F_{CH_4,eq}$ on maximum temperature gradient and maximum cell temperature of the solid part in SOFC fed by different types of feed. The increase in $F_{CH_4,eq}$ can decrease both maximum temperature gradient and maximum temperature in SOFC cell. This is due to the fact that fuel utilization and also the irreversibility are very high for SOFC with low feed rate and they decrease as $F_{CH_4,eq}$ increases as illustrated in Fig. 4b. However, for SOFC fed by biogas, severe decrease in fuel utilization, maximum temperature gradient and maximum cell temperature with the increase in $F_{CH_4,eq}$ can be found at around 3×10^{-4}–4×10^{-4} mol s^{-1}. It can be explained by the fact that CH_4 in biogas cannot be entirely reformed when $F_{CH_4,eq}$ is higher than 3×10^{-4} mol s^{-1}. The optimum power density can be obtained when $F_{CH_4,eq}$ is well tuned up. When the feed rate is low, the increase in feed rate can improve the power density because the fuel utilization does not significantly decrease with the feed velocity. However, for SOFC with high feed rate, the fuel utilization significantly drops as the feed velocity increases while the power density does not significantly decrease with the increase of feed rate. These results imply that $F_{CH_4,eq}$ should be carefully considered to achieve a suitable value. With low $F_{CH_4,eq}$, the solid part in SOFC cell may be damaged due to extremely high temperature. However, with excessively high $F_{CH_4,eq}$, fuel utilization and power density of SOFC may be inhibited. The study on the effect of the change in feed flow rate on the electrical efficiency (Fig. 4c) also indicates that the intermediate fuel flow rate is preferred. Optimum electrical efficiency is found and does not change with feed velocity at low to intermediate fuel feed rates, however, when operating at high fuel velocities, it decreases as the fuel feed rate increases.

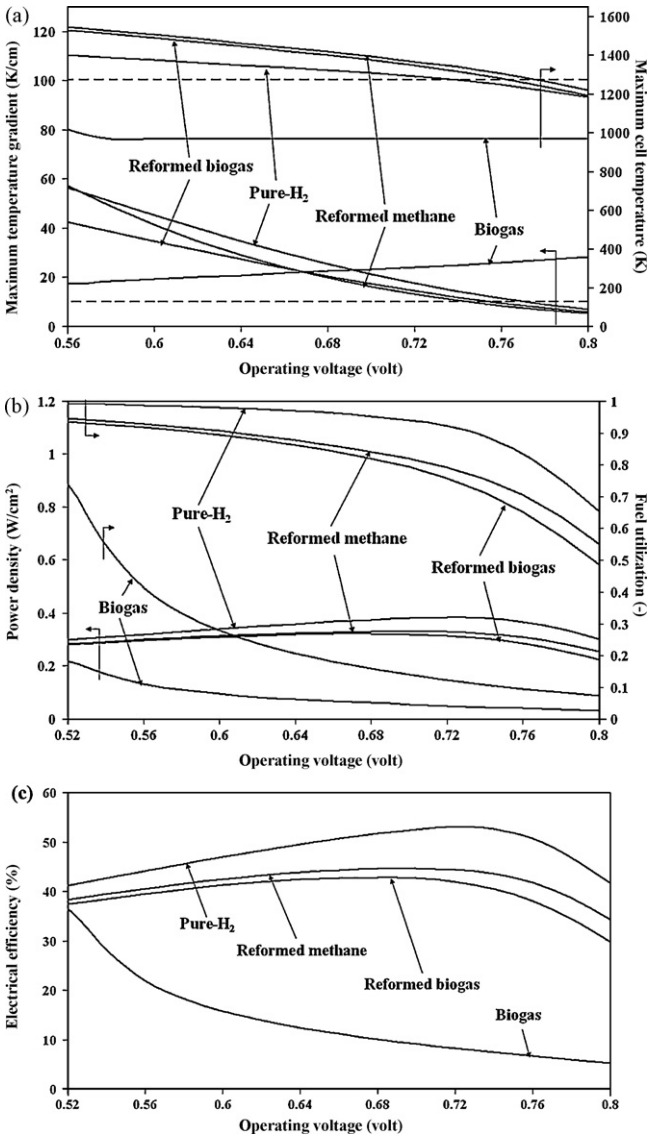

Fig. 5. The effect of the change in operating voltage on (a) the maximum temperature gradient, maximum cell temperature, (b) power density, fuel utilization and (c) electrical efficiency for SOFC fed by different types of feed in case that $F_{CH_4,eq}$ is equal to 3×10^{-4} mol s^{-1}. (Excess air is equal to base case values.)

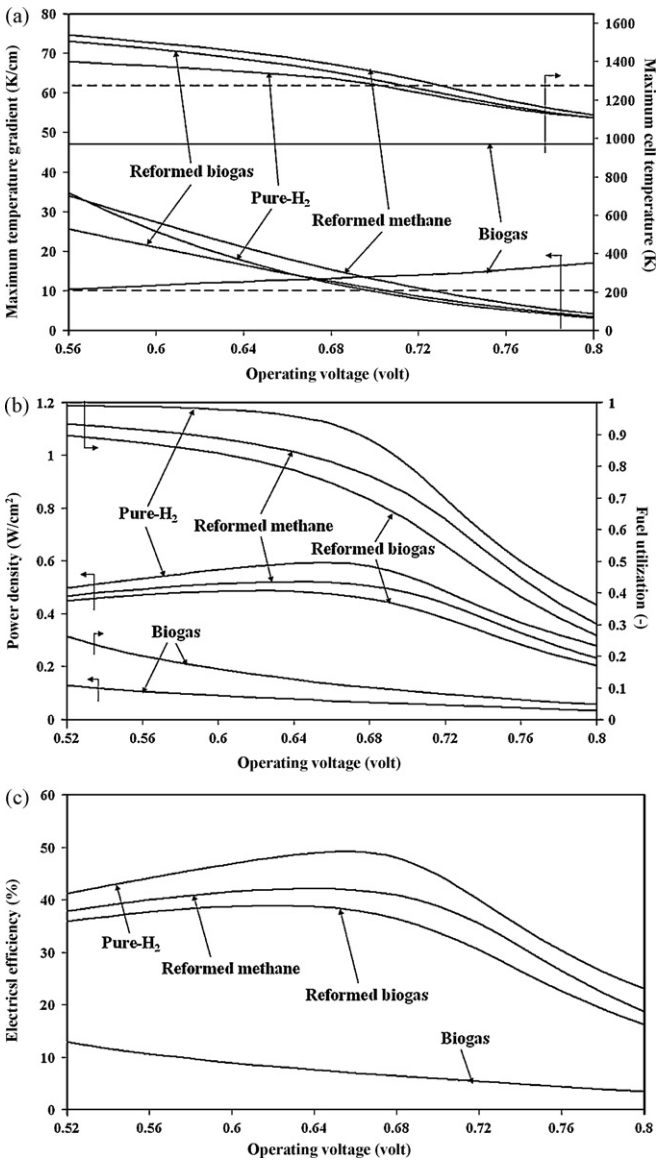

Fig. 6. The effect of the change in operating voltage on (a) the maximum temperature gradient, maximum cell temperature, (b) power density, fuel utilization and (c) electrical efficiency for SOFC fed by different types of feed in case that $F_{CH_4,eq}$ is equal to 5×10^{-4} mol s^{-1}. (Excess air is equal to base case values).

To compare the performance of SOFC fed by different feed, the effects of the operating voltage on the maximum temperature gradient, maximum cell temperature, power density, fuel utilization and electrical efficiency were investigated as shown in Figs. 5 and 6 for $F_{CH_4,eq}$ of 3×10^{-4} and 5×10^{-4} mol s^{-1}, respectively. The excess air is kept to be constant at the base case of 400% excess. The dash lines in Figs. 5a and 6a represent the maximum acceptable temperature gradient (MATG), 10 K cm^{-1}, and maximum acceptable cell temperature (MACT), 1273 K. As shown in Figs. 5a and 6a, excluding SOFC fed by biogas, the increase in operating voltage can improve the operation viability of SOFC. As the operating voltage increases, heat generation caused from the irreversibility is reduced and the cell temperature drops. Inversely, for SOFC fed by biogas, the operation at low operating voltage is preferred since large amount of heating energy generated from the irreversibility can be used in endothermic methane steam reforming and the decreasing rate of cell temperature in the flow direction is reduced. The results in Figs. 5a and 6a also imply that it is difficult to operate SOFC fed by biogas at excess air lower than 400% since the maximum temperature gradient and maximum cell temperature would increase. Moreover, as illustrated in Figs. 5b, 5c, 6b and 6c, the fuel utilization, power density and electrical efficiency of SOFC fed by biogas are significantly lower than those of SOFC fed by the other feeds. Therefore, it can be concluded that direct biogas feed is not a recommended feedstock for SOFC. The operation at high operating voltage is desired to minimize the temperature and temperature gradient of solid part in SOFC. However, the fuel utilization obtained at this condition is not satisfied, as shown in Figs. 5b and 6b, the fuel utilization decreases as the operating voltage increases. When operating at the same operating voltage, SOFC fed by pure-H_2 offers higher fuel utilization compared with SOFC fed by the other feed types. This implies that H_2 concentration is the important factor which affects the rate of electrochemical reaction. The optimum operating voltage which offers maximum power density can be observed as illustrated in Figs. 5b and 6b. When the operating voltage is lower than the optimum value, the increase in operating voltage can improve the power density since fuel utilization does not significantly decrease. The pronounced decrease in fuel utilization with the increase in operating voltage can be found as the operating volt-

Table 3
Summary of SOFC fed by different feed operating at the optimum operating condition in case that $F_{CH_4,eq}$ and excess air are equal to 3×10^{-4} mol s^{-1} and 400%, respectively.

Type of feed	Biogas	Biogas-reformed feed	Methane-reformed feed	Pure-H_2
$F_{CH_4,eq}$ (mol s^{-1})	0.0003	0.0003	0.0003	0.0003
Excess air (%)	400	400	400	400
Operating voltage (V)	n.a.	0.764	0.778	0.746
Power density (W cm^{-1})	n.a.	0.282	0.29	0.379
Current density (A cm^{-1})	n.a.	0.369	0.373	0.508
Electrical efficiency (%)	n.a.	37.48	39.13	52.20
U_f	n.a.	0.638	0.645	0.877
Electricity produced (W)	n.a.	112.82	116.14	151.48
Maximum temperature gradient (K cm^{-1})	n.a.	9.09	9.21	9.95
Maximum cell temperature (K)	n.a.	1272.06	1271.71	1267.26

Table 4
Summary of SOFC fed by different feed operating at the optimum operating condition in case that $F_{CH_4,eq}$ and excess air are equal to 5×10^{-4} mol s^{-1} and 400%, respectively.

Type of feed	Biogas	Biogas-reformed feed	Methane-reformed feed	Pure-H_2
$F_{CH_4,eq}$ (mol s^{-1})	0.0005	0.0005	0.0005	0.0005
Excess air (%)	400	400	400	400
Operating voltage (V)	0.48	0.715	0.732	0.704
Power density (W cm^{-1})	0.167	0.393	0.407	0.532
Current density (A cm^{-1})	0.349	0.55	0.556	0.755
Electrical efficiency (%)	16.69	31.35	32.91	43.97
U_f	0.366	0.57	0.577	0.783
Electricity produced (W)	66.97	157.27	162.79	212.69
Maximum temperature gradient (K cm^{-1})	9.74	9.09	9.35	9.38
Maximum cell temperature (K)	1030.88	1271.67	1271.80	1272.52

age is higher than the optimum value; hence, power density also decreases. The change in electrical efficiency with the operating voltage is in the same tendency as the change in power density as shown in Figs. 5c and 6c.

Tables 3 and 4 summarize the optimum operating condition of SOFC fuelled by each feed type for $F_{CH_4,eq} = 3 \times 10^{-4}$ and 5×10^{-4} mol s^{-1}, respectively. These results imply that, with the same cell dimension, excess air and $F_{CH_4,eq}$, SOFC fed by pure-H_2 feed offers higher power density than SOFC fed by the other fuel types. For $F_{CH_4,eq}$ of 3×10^{-4} and 5×10^{-4} mol s^{-1}, power density of SOFC fuelled by pure-H_2 is 0.379 and 0.532 W cm^{-2}, respectively. Also, the values of electrical efficiency of 52.20 and 43.97% are achieved for SOFC fed by pure-H_2 with $F_{CH_4,eq}$ of 3×10^{-4} and 5×10^{-4} mol s^{-1}, respectively. Methane-reformed feed is fairly better than biogas-reformed feed due to its higher hydrogen concentration. With excess air of 400%, biogas-fed SOFC is not viable to operate when $F_{CH_4,eq}$ is equal to 3×10^{-4} mol s^{-1}. On the other hand, at 5×10^{-4} mol s^{-1} of $F_{CH_4,eq}$ the SOFC fed by biogas offers extremely lower power density (0.167 W cm^{-2}) compared with the other feeds.

4. Conclusion

Mathematical model of SOFC has been developed for investigating operation viability and performance of SOFC fed by different feeds. Four types of fuel feed, i.e. biogas, biogas-reformed feed, methane-reformed feed and pure-H_2, are considered in this study. In operation viability investigation, maximum temperature gradient and maximum cell temperature are employed as the indicators. Additionally, power density and electrical efficiency are considered as performance indicators. The effect of the change in operating conditions, i.e. excess air, fuel feed rate and operating voltage, are also investigated. The increase in excess air can improve the operation viability of SOFC; however, with surplus excess air, its power density is inhibited. Also, the operation of SOFC is viable at high fuel feed rate. Nevertheless, excess high fuel feed rate is not favored since the SOFC cell could be saturated with current, resulting in the dropping of the fuel utilization. Excluding SOFC fed by biogas, SOFC becomes operation viable as it operates at high operating voltage. Inversely, for biogas-fuelled SOFC, the operation at low operating voltage is preferred in thermal management point of view. The optimum operating voltage which offers utmost power density can be observed. Conclusively, the value of excess air, fuel feed rate and operating voltage should be carefully adjusted to obtain best possible power density and reasonable temperature and temperature gradient. SOFC fed by pure-H_2 offers highest power density compared with that fed by the other feeds. Biogas-fed SOFC can become operation viable as it operates at high excess air; nevertheless, its power density is extremely lower than SOFC fuelled by the other feeds. Methane-reformed feed offers higher SOFC power density compared with biogas-reformed feed since its H_2 concentration is higher. Although pure-H_2 is an attractive fuel for SOFC, the transformation process of a primary fuel to H_2 should also be received the attention.

Acknowledgement

The support from The Thailand Research Fund and Commission on Higher Education is gratefully acknowledged.

References

[1] R.J. Spiegel, J.L. Preston, Test results for fuel cell operation on anaerobic digester gas, J. Power Sources 86 (2000) 283–288.
[2] S. Baron, N. Brandon, A. Atkinson, B. Steele, R. Rudkin, The impact of wood-derived gasification gases on Ni-CGO anodes in intermediate temperature solid oxide fuel cells, J. Power Sources 126 (2004) 58–66.
[3] V.M. Janardhanan, V. Heuveline, O. Deutschmann, Performance analysis of a SOFC under direct internal reforming conditions, J. Power Sources 172 (2007) 296–307.
[4] P. Piroonlerkgul, S. Assabumrungrat, N. Laosiripojana, A.A. Adesina, Performance of biogas-fed solid oxide fuel cell system integrated with membrane module for CO_2 removal, Chem. Eng. Process.: Process Intensification 48 (2009) 672–682.
[5] R. Suwanwarangkul, E. Croiset, E. Entchev, S. Charojrochkul, M.D. Pritzker, M.W. Fowler, P.L. Douglas, S. Chewathanakup, H. Mahaudom, Experimental and modeling study of solid oxide fuel cell operating with syngas fuel, J. Power Sources 161 (2006) 308–322.
[6] W. Sangtongkitcharoen, S. Vivanpatarakij, N. Laosiripojana, A. Arpornwichanop, S. Assabumrungrat, Performance analysis of methanol-fueled solid oxide fuel cell system incorporated with palladium membrane reactor, Chem. Eng. J. 138 (2008) 436–441.

[7] L.T. Lim, D. Chadwick, L. Kershenbaum, Achieving autothermal operation in internally reformed solid oxide fuel cells: simulation studies, Ind. Eng. Chem. Res. 44 (2005) 9609–9618.
[8] M. Sorrentino, C. Pianese, Y.G. Guezennec, A hierarchical modeling approach to the simulation and control of planar solid oxide fuel cells, J. Power Sources 180 (2008) 380–392.
[9] P. Aguiar, D. Chadwick, L. Kershenbaum, Modelling of an indirect internal reforming solid oxide fuel cell, Chem. Eng. Sci. 57 (2002) 1665–1677.
[10] P. Aguiar, D. Chadwick, L. Kershenbaum, Effect of methane slippage on an indirect internal reforming solid oxide fuel cell, Chem. Eng. Sci. 59 (2004) 87–97.
[11] M.A. Khaleel, Z. Lin, P. Singh, W. Surdoval, D. Collin, A finite element analysis modeling tool for solid oxide fuel cell development: coupled electrochemistry, thermal and flow analysis in MARC(R), J. Power Sources 130 (2004) 136–148.
[12] R. Blom, I.M. Dahl, A. Slagtem, B. Sortland, A. Spjelkavik, E. Tangstad, Carbon dioxide reforming of methane over lanthanum-modified catalysts in a fluidized-bed reactor, Catal. Today 21 (1994) 535–543.
[13] M.C.J. Bradford, M.A. Vannice, Catalytic reforming of methane with carbon dioxide over nickel catalysts. II. Reaction kinetics, Appl. Catal. A: Gen. 142 (1996) 97–122.
[14] H.M. Swaan, V.C.H. Kroll, G.A. Martin, C. Mirodatos, Deactivation of supported nickel catalysts during the reforming of methane by carbon dioxide, Catal. Today 21 (1994) 571–578.
[15] E. Achenbach, E. Riensche, Methane/steam reforming kinetics for solid oxide fuel cells, J. Power Sources 52 (1994) 283–288.
[16] P. Piroonlerkgul, S. Assabumrungrat, N. Laosiripojana, A.A. Adesina, Selection of appropriate fuel processor for biogas-fuelled SOFC system, Chem. Eng. J. 140 (2008) 341–351.
[17] F. Zhao, A.V. Virkar, Dependence of polarization in anode-supported solid oxide fuel cells on various cell parameters, J. Power Sources 141 (2005) 79–95.
[18] P. Aguiar, C.S. Adjiman, N.P. Brandon, Anode-supported intermediate temperature direct internal reforming solid oxide fuel cell. I. Model-based steady-state performance, J. Power Sources 138 (2004) 120–136.
[19] M. Ni, M.K.H. Leung, D.Y.C. Leung, Parametric study of solid oxide fuel cell performance, Energy Convers. Manage. 48 (2007) 1525–1535.